

Bacteriophage-mediated interference of the c-di-GMP signalling pathway in *Pseudomonas aeruginosa*

Jeroen De Smet,^{1,†}  Jeroen Wagemans,¹ 
Hanne Hendrix,¹  Ines Staes,² Annegrete
Visnapuu,¹ Benjamin Horemans,³ Abram
Aertsen,²  and Rob Lavigne¹ 

¹Laboratory of Gene Technology, Department of Biosystems, KU Leuven, Heverlee, 3001, Belgium.

²Laboratory of Food Microbiology, Department of Microbial and Molecular Systems, KU Leuven, Heverlee, 3001, Belgium.

³Department of Earth and Environmental Sciences, KU Leuven, Heverlee, 3001, Belgium.

Summary

C-di-GMP is a key signalling molecule which impacts bacterial motility and biofilm formation and is formed by the condensation of two GTP molecules by a diguanylate cyclase. We here describe the identification and characterization of a family of bacteriophage-encoded peptides that directly impact c-di-GMP signalling in *Pseudomonas aeruginosa*. These phage proteins target *Pseudomonas* diguanylate cyclase YfiN by direct protein interaction (termed YIPs, YfiN Interacting Peptides). YIPs induce an increase of c-di-GMP production in the host cell, resulting in a decrease in motility and an increase in biofilm mass in *P. aeruginosa*. A dynamic analysis of the biofilm morphology indicates a denser biofilm structure after induction of the phage protein. This intracellular signalling interference strategy by a lytic phage constitutes an unexplored phage-based mechanism of metabolic regulation and could potentially serve as inspiration for the development of molecules that interfere with biofilm formation in *P. aeruginosa* and other pathogens.

Received 11 August, 2020; revised 19 October, 2020; accepted 22 November, 2020.

For correspondence: E-mail rob.lavigne@kuleuven.be; Tel. +32 16379524; Fax +32 16321965.

Present address: Lab4Food, Department of Microbial and Molecular Systems (M2S), KU Leuven Campus Geel, Geel, 2440, Belgium.

Microbial Biotechnology (2021) 14(3), 967–978

doi:10.1111/1751-7915.13728

Funding Information This work was in part supported by a GOA grant 'Phage biosystems' (GOA/15/006) from KU Leuven. J.D.S. holds a postdoctoral fellowship grant (grant number: 12V5219N) of the Research Foundation – Flanders. I.S. and A.V. hold a 'strategic basic research' PhD fellowship (grant numbers: 1S56416N and 1S44616N, respectively) of the Research Foundation – Flanders.

Introduction

Cyclic dinucleotides are among the most widespread signalling molecules used by organisms, converting extra-/intracellular stimuli into metabolic changes by mostly binding as an allosteric regulator to effector molecules (Pesavento and Hengge, 2009). Bis-(3'5')-cyclic diguanosine monophosphate (c-di-GMP) was the first one to be described in 1987 (Ross *et al.*, 1987). In recent years, c-di-GMP has emerged as a key regulator of numerous processes including in transitions between planktonic and sessile lifestyles, in cell differentiation and in virulence (Hengge, 2009, 2016; Römling *et al.*, 2013). C-di-GMP is formed by the condensation and cyclization of two molecules of GTP by diguanylate cyclase enzymes (DGCs), containing a GGDEF motif, and is degraded by phosphodiesterases (PDEs), containing an EAL or HD-GYP motif (Simm *et al.*, 2004). In *P. aeruginosa* strain, PAO1 at least 41 proteins are predicted to be involved in c-di-GMP signalling, illustrating its central role in this organism (Kulasakara *et al.*, 2006; Seshasayee *et al.*, 2010).

Originally, it was proposed that high intracellular levels of c-di-GMP are linked with biofilm formation, whereas low levels result in increased motility (Baraquet and Harwood, 2013; Martinez-Granero *et al.*, 2014). While this remains the general concept, a far more intricate regulation mechanism behind the regulation of intracellular c-di-GMP concentration levels and its impact on bacterial processes has emerged (Hengge, 2009; Valentini and Filloux, 2016). For example, during biofilm formation the binding to a surface coincides with a loss of motility caused by a DGC (SadC) and an increased exopolysaccharide production, caused by a second DGC (RoeA) (Merritt *et al.*, 2007, 2010). Although both DGCs increase the c-di-GMP level, they exert different effects on the cell. This is presumably due to the localized activity of DGCs and PDEs causing intracellular differences in c-di-GMP levels (Christen *et al.*, 2010; Massie *et al.*, 2012). Another example of the complexity of c-di-GMP regulated responses is observed during induction of biofilm dispersion in *P. aeruginosa*, upon nitrous oxide or glutamate exposure. The response to nitrous oxide and glutamate signals is mediated through protein BdlA, which undergoes c-di-GMP-dependent proteolysis in response to a rapid increase in c-di-GMP level by two DGCs (NicD and GcbA) (Petrova and Sauer, 2012).

Cleaved BdlA will in turn activate the PDEs DipA and RbdA. The resulting degradation of c-di-GMP causes the dispersion of cells from the biofilm, within a fifteen minutes timeframe following the exposure to glutamate (Basu and Sauer, 2014; Petrova *et al.*, 2015). Since many DGCs and PDEs are still uncharacterized, it is expected that more elaborate mechanisms of c-di-GMP regulation will be unveiled.

These complex regulation mechanisms do offer opportunities to hijack the control over this important signalling pathway in many bacterial pathogens, including some of the so-called 'priority' pathogens. Since biofilms reduce antibiotic treatment efficacy and impact antibiotic resistance development in bacteria, c-di-GMP-based regulation of biofilm formation is explored as an alternative target for antibacterial treatment (Jimenez *et al.*, 2012; Ryan, 2013; Caly *et al.*, 2015; Hee *et al.*, 2020). In this regard, bacterial viruses are valuable sources for novel bacterial control strategies, as bacteriophages specifically infect their host and hijack cellular activities for the production of phage progeny (De Smet *et al.*, 2017). To optimize this process, phage proteins perform specialized functions with sometimes massive effects on the host cell (Van den Bossche *et al.*, 2014; Wagemans *et al.*, 2014, 2015). The lack of functional predictions for these uncharacterized proteins suggests a potentially vast repository of molecular tools for antibacterial and biotechnological applications (De Smet *et al.*, 2017; Wan *et al.*, 2020).

Here, we identify and characterize a family of small c-di-GMP interfering peptides encoded by PB1-like *Pseudomonas* phages. These phages, belonging to the *Myoviridae* phage family, are widespread in nature and expected to bind the lipopolysaccharide layer as receptor (Ceyssens *et al.*, 2009; Garbe *et al.*, 2010). The studied peptides are identified in a screen for growth-inhibitory proteins from *Pseudomonas* phages, impacting the *P. aeruginosa* morphology and inducing small colony variants. We provide evidence that this phenotype is the result of increased c-di-GMP levels due to a direct interaction of the phage peptides with diguanylate cyclase YfiN (also called TpbB or PA1120). Expression of these YfiN interacting peptides (YIPs) affects c-di-GMP regulated processes, including cellular motility and biofilm

formation, which are restored in *yfiN* transposon deletion mutants, illustrating the extensive impact of the peptides on host metabolism. This study unveils a natural phage-induced interference mechanism to manipulate host signalling pathways as a novel host–parasite hijacking strategy.

Results

The PB1-like viruses encode a protein family of YfiN interacting peptides which alter P. aeruginosa colony morphology

A screen of 38 ORFans, encoded by the early genome region of three *Pbunavirus* members 14-1, LMA2 and LBL3, revealed only a limited number of proteins that have an inhibitory effect on *P. aeruginosa* PAO1 growth (solid and liquid medium) when expressed from an integrated vector pUC18mini-Tn7T-Lac-GW, one of which (14-1 gp12) was previously identified as a transcription inhibitor (Van den Bossche *et al.*, 2014). The remaining three proteins impact the colony morphology of both the PAO1 and PA14 *P. aeruginosa* strains. These proteins are close homologs of each other, LBL3 gp88 (YP_004221739) and LMA2 gp93 (YP_004221740) share 100% sequence similarity, while 14-1 gp11 (YP_002364319) only differs at three amino acids (Fig. 1). In fact, homologs of these peptides are identified in 97 *Pbunavirus* phages using tBLASTx (Zhang *et al.*, 2000), while at the same time no similarity is identified with any other sequence (Table S1). Bioinformatic analysis also predicts that these peptides (referred to hereafter as YIPs) have the potential to form transmembrane helices (Fig S1). Due to their small size (3.58 kDa), YIPs are likely to exert their effect on *P. aeruginosa* growth via a protein–protein interaction.

To search for interaction partners within the host, a Yeast Two-Hybrid (Y2H) screen was set up using LBL3 YIP as bait against a random fragment prey library of the *P. aeruginosa* PAO1 genome (Roucourt *et al.*, 2009). No autoactivation by the bait protein was observed. The interaction screen generated a number of potential partners (Table S2). The enriched targets (YfiN, PctB, FimV and NarX) were therefore tested in an independent Y2H experiment using fresh yeast cells (Fig. S2A). Moreover, the

LBL3 gp88	MIYTTIKAMAWFALLWATGLSIVTLTIHFCY	31
LMA2 gp93	MIYTTIKAMAWFALLWATGLSIVTLTIHFCY	31
14-1 gp11	MIYITIKAMAWFALLWATGLAIVTLTIHLCY	31
	*** ***** . ***** .**	

Fig. 1. Sequence comparison between LBL3 gp88/YIP, LMA2 gp93/YIP and 14-1 gp11/YIP using Clustal Omega (Madeira *et al.*, 2019). An asterisk indicates positions with conserved residues. A colon indicates a conservation between a group of similar amino acids. The length of the gene products are indicated after the sequence.

specificity of these interactions was examined using non-related bait and prey constructs (Fig. S2). The YfiN (PA1120) - LBL3 YIP and FimV (PA3115) - LBL3 YIP interactions were reproducible and specific, confirming that YfiN and FimV are potential interaction partners of the LBL3 protein. YfiN (also known as TpbB) is a diguanylate cyclase, characterized by the highly conserved GGDEF domain, involved in the synthesis of c-di-GMP. In total, two different interacting prey constructs (Table S2) were retrieved, both containing a fragment consisting of the first 200 amino acids of YfiN. This region forms two transmembrane (TM) helices and the periplasmic Cache domain (Giardina *et al.*, 2013; Hengge *et al.*, 2016). FimV, on the other hand, is an inner membrane protein, that regulates intracellular cyclic AMP (cAMP) levels and thus type IV pilus-mediated twitching, arising from extension and retraction of pili from their site of assembly in the inner membrane (Wehbi *et al.*, 2011; Buensuceso *et al.*, 2016).

To obtain evidence that the interactions between the phage proteins and the identified interaction partners are responsible for the observed biological phenotype, YIPs were expressed in transposon mutants of *yfiN* and *fimV* (Fig. 2 and Fig. S3). In both the wild-type PAO1 and PA14 *P. aeruginosa* strains, expression of an individual YIP gene leads to a compact colony with no apparent swarming, a phenotype that was initially confused with a growth-inhibitory effect on plate. This phenotype is also observed in the transposon mutant of *fimV*. The deletion of *yfiN*, on the other hand, effectively abolishes this morphology and restores normal growth, corroborating the connection between YfiN and YIPs 14-1 gp11 or LBL3

gp88 and their effect on bacterial motility. Based on this interaction analysis, we dubbed the 14-1, LBL3 and LMA2 proteins as YIP for 'YfiN Interacting Peptide'.

Expression of YIP results in increased intracellular c-di-GMP levels

To investigate how YIP interferes with the function of YfiN, the level of c-di-GMP was measured using a *P. aeruginosa* strain in which a c-di-GMP-responsive promoter (pCdrA) is fused to a GFP reporter gene (Rybtko *et al.*, 2012). This construct allows the correlation of the level of fluorescence to the amount of c-di-GMP produced. This fluorescent signal is observed microscopically and quantified using MicrobeTracker (Sliusarenko, 2012) (Fig. 3). Induction of YIP with IPTG affects the level of fluorescence resulting in a small upwards shift in intensity compared to the controls. After 1.5 h of induction, the intensity of fluorescence doubled in 43% of the cells, compared to 1.8% of the cells of the induced control strain (Fig. 3). This rapid and strong increase in c-di-GMP levels, induced by YIP, is expected to have major implications on bacterial phenotypic properties.

Expression of YIP results in increased biofilm formation and reduced motility

Increased c-di-GMP levels are reported to lead to reduced motility and increased biofilm formation (Hengge, 2009; Römling *et al.*, 2013). To investigate this

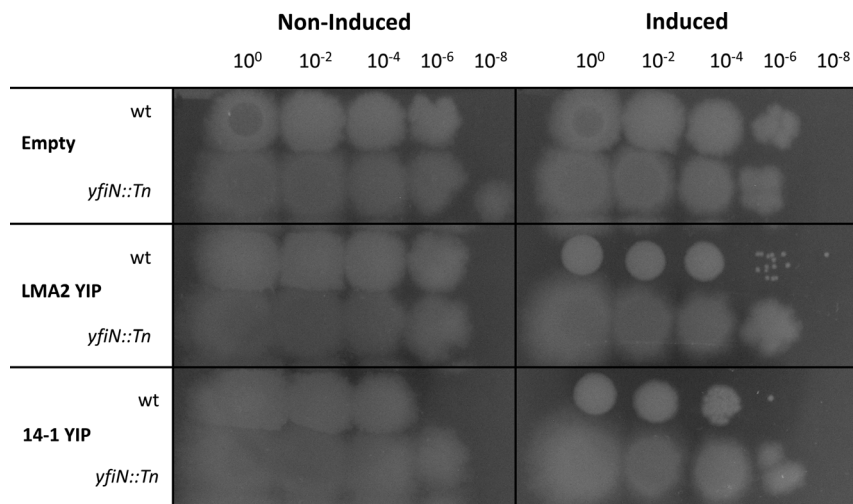


Fig. 2. Impact of YIP on bacterial growth in PAO1 wild type (wt) and a transposon mutant of *yfiN* (*yfiN::Tn*). Hundredfold serial dilutions of *P. aeruginosa* PAO1 cells containing a single-copy integration of the YIP gene under control of an IPTG-inducible promoter, were spotted on LB agar without (left) or with (right) 1 mM IPTG and grown for 16 h at 37°C. As a negative control, a *P. aeruginosa* PAO1 strain encoding an empty pUC18-mini-Tn7T-Lac expression cassette was used. Both YIP proteins trigger the same phenotypic effect of reduced spreading of the colony. The observed phenotypic effect of the YIP proteins is absent in the PAO1 transposon mutant of YfiN, showing that this protein is indeed the direct target of YIP.

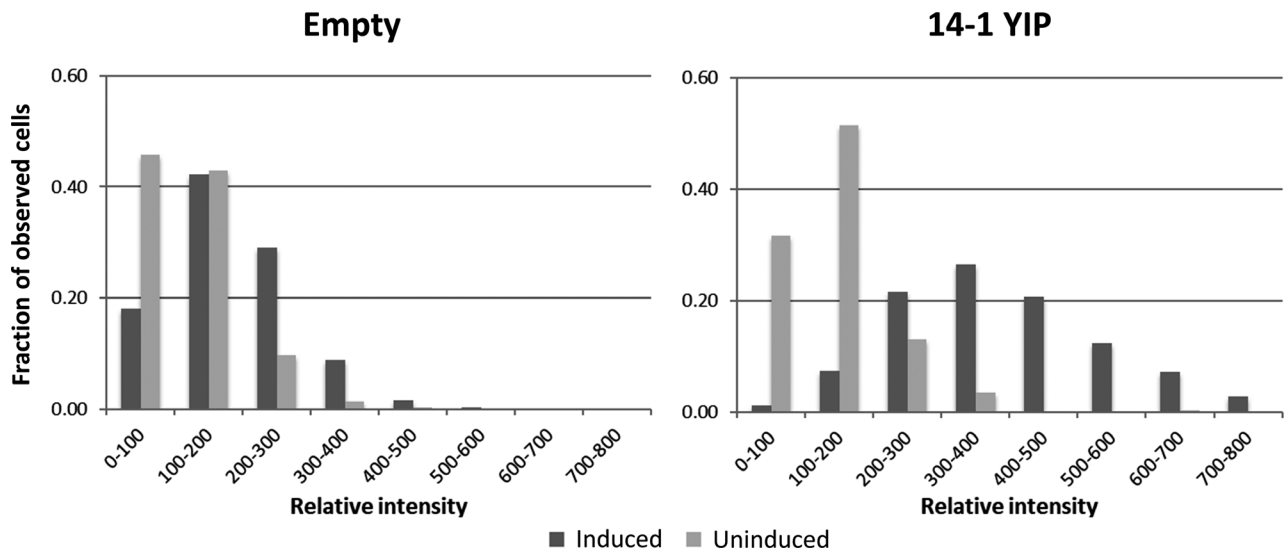


Fig. 3. YIP increases c-di-GMP production in PAO1. Using a *P. aeruginosa* strain containing a GFP expression construct under control of a c-di-GMP-responsive promoter, the c-di-GMP level was measured after 1.5 h of induction of YIP (1 mM IPTG).

for the YIP proteins, a swarming and swimming motility assay was performed that revealed a reduction in the swarming and swimming motility for both YIP homologs tested (Fig. 4A and B). The impact on the twitching motility of the 14-1 YIP was also analysed, revealing a clear reduction in twitching motility as well (Fig. 4B). Upon induction of the YIP homolog, the diameter of the twitching motility zone decreased from 1.72 to 0.82 cm, which was not the case for the control. Also, the Calgary device was used to explore the impact of YIP on biofilm formation both in the *P. aeruginosa* PAO1 wild-type strain and the transposon deletion mutant of *yfiN* (Fig. 4C). Biofilm formation is clearly reduced in the transposon mutant of *yfiN*, with about half the amount of biofilm formed compared to the wild type. The expression of YIP does not have an effect on biofilm formation in the mutant strain. In contrast, the wild type shows a 25% increase in biofilm formation after 24 h upon expression of YIP. Hence, both the motility and biofilm formation assay support our findings that the YIP phage proteins interfere with c-di-GMP signalling through YfiN and result in an increased production of this signal molecule.

Expression of YIP alters the three-dimensional structure of the biofilm structures formed

Representative three-dimensional (3D) views of a dynamic *P. aeruginosa* PAO1 wild-type biofilm with or without expression of 14-1 YIP analysed by confocal laser scanning microscopy (CLSM) are shown in Fig. 4D. After four days without YIP induction, *P. aeruginosa* PAO1 developed large mounds with layers of cells

between most of these mounds leading to an almost complete coverage of the surface, a typical stage in the development of flat-layered PAO1 biofilms (Klausen *et al.*, 2003). In contrast, when 14-1 YIP was induced, smaller mounds developed with no layering of cells between these mounds. Klausen *et al.* (2003) previously showed that twitching motility plays a role in the formation of flat-layered PAO1 biofilms starting from the mounds formed by local cell proliferation. Indeed, for wild-type *P. aeruginosa* cells the combination of growth and migration, through Type IV pili-mediated twitching, is needed to form these flat-layered biofilms, while the combination of growth and non-motility will lead to the creation of protruding structures in the biofilm of $\Delta pila$ mutants. One potential explanation for the involvement of Type IV pili in the motility of cells through the biofilm structure during maturation are the identified interactions of the pili with extracellular DNA (van Schaik *et al.*, 2005).

To conclude, the observations of Klausen *et al.* (2003) do align with ours when 14-1 YIP is expressed. This confirms our findings that the interaction of 14-1 YIP with YfiN leads to an increase in intracellular c-di-GMP levels (Fig. 3), this in turn inhibits the twitching motility of the *P. aeruginosa* cells (Fig. 4B) and thus the observed biofilm phenotype of localized, dense mounds (Fig. 4D). Interestingly, Klausen *et al.* (2003) also reported an increase in biomass accumulation for the $\Delta fliM$ and $\Delta pila\Delta fliM$ biofilms, which they linked to a selective advantage for non-flagellated variants. A similar increased biomass formation was also observed in this study for the wild-type biofilm with 14-1 YIP expression under static conditions (Fig. 4C).

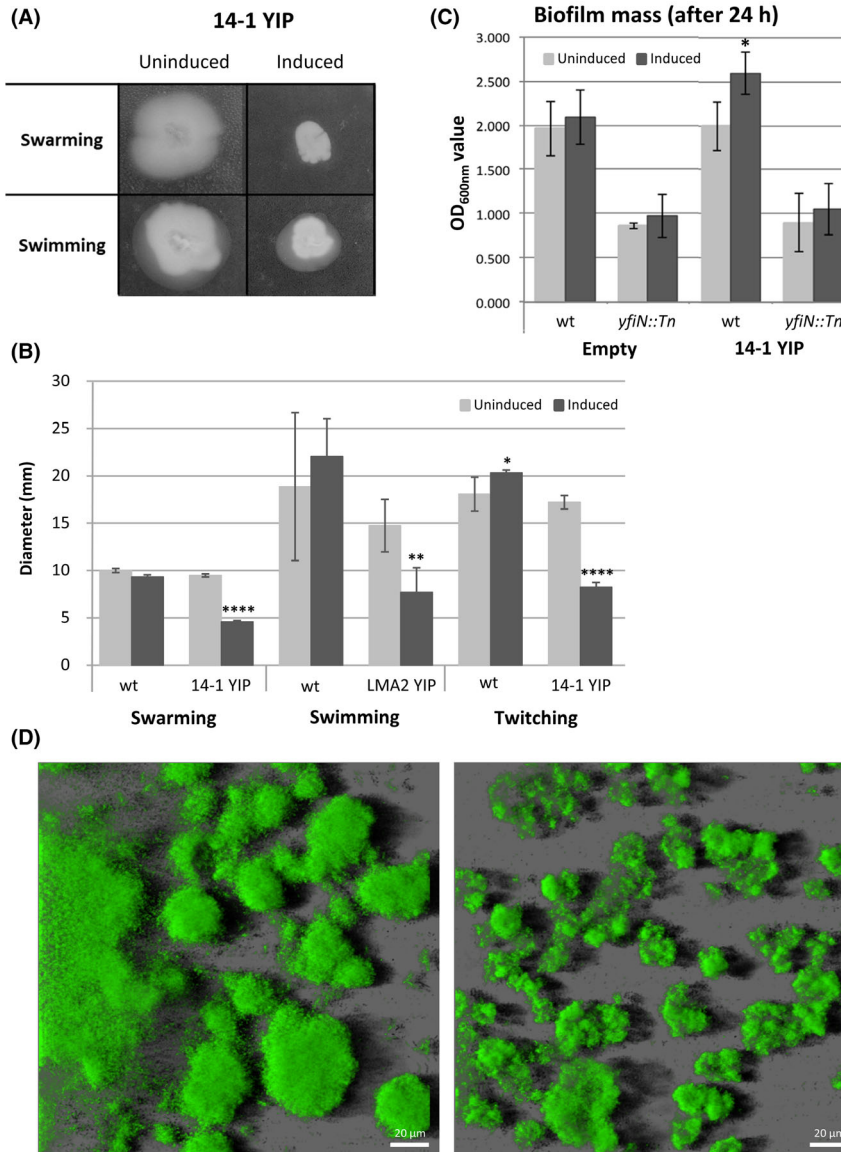


Fig. 4. YIP inhibits motility and increases the amount of biofilm formed in *P. aeruginosa* PAO1.A. Picture of result of motility assays for 14-1 YIP (plates were incubated for 24 h at 37°C).B. Graphic representation of motility assays for YIP that show a clear reduction upon induction. Error bars represent standard deviations, and *P*-values were calculated using Student's t-test (swimming, *n* = 3; swarming and twitching, *n* = 5), **P* < 0.05, ***P* < 0.01, *****P* < 0.0001. wt, PAO1::Empty.C. Using a Calgary device the impact of 14-1 YIP on the biofilm mass formed after 24 h was measured in both wild-type (wt) PAO1 and a transposon mutant of *yfiN* (*yfiN*::*Tn*) (right, 14-1 YIP) and compared with both PAO1 strains encoding the empty expression cassette (left, Empty). Standard deviations and *p*-values are indicated (*n* = 12), **P* < 0.05.D. Representative 3D images of biofilms formed in flow channels under dynamic conditions. Continuous flow channels were inoculated with *P. aeruginosa* PAO1 (in green) with or without the 14-1 YIP expression construct and were incubated for four days, continuously fed with minimal medium for *Pseudomonas* supplemented with 1 mM IPTG at a flow rate of 3.5 ml h⁻¹. (left panel) 3D image of biofilm from *P. aeruginosa* PAO1::Empty with induction; and (right panel) 3D image of biofilm from *P. aeruginosa* PAO1::14-1 YIP with induction.

Discussion

A novel mode of phage-induced c-di-GMP signalling interference

The protein YfiN is involved in the quorum sensing control of biofilm formation through the *pel* locus (Ueda and Wood, 2009). It has been experimentally identified as a

membrane-bound diguanylate cyclase (Kulasakara *et al.*, 2006; Malone *et al.*, 2010). It is part of the *yfiBNR* operon, where the small periplasmic protein, YfiR (PA1121), negatively regulates YfiN and the OmpA/Pal-like outer-membrane lipoprotein YfiB counteracts this effect (Giardina *et al.*, 2013). Stress-induced depression results in a conformational change within YfiN (Fig. 5,

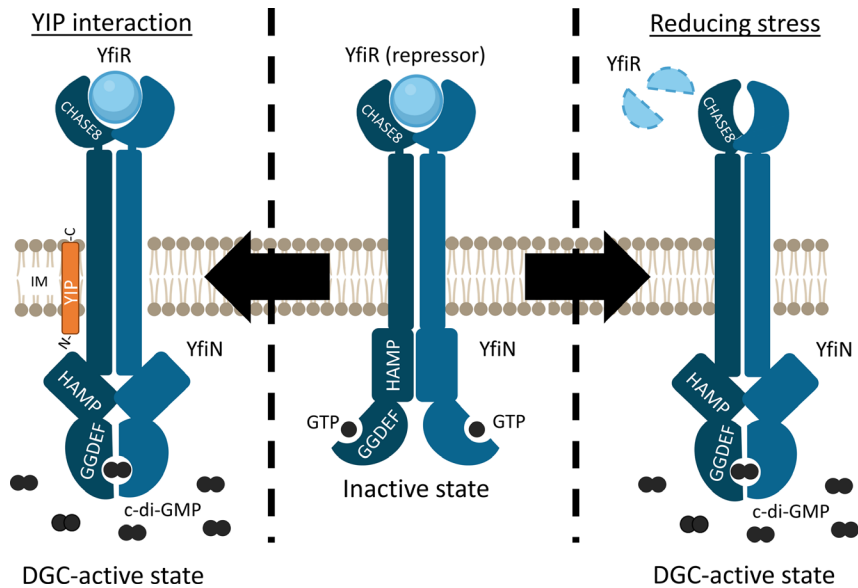


Fig. 5. Schematic representation of the putative allosteric regulation of YfiN based on homology modelling and the hypothesized mode of action of YIP. Interaction with YfiR will block YfiN in the inactive conformation (middle panel). Only when YfiR is removed either by binding to YfiB or degradation, conformational changes will occur and reveal the catalytic GGDEF site (right panel). The interaction with YIP will trigger a similar conformational change in YfiN (left panel).

right panel). According to the study of Giardina *et al.* (2013), the two arms of the PAS domain, since then reclassified as a CHASE8 domain, push the TM2 helices towards the cytosolic side of the inner membrane, a movement which is transmitted through torsion of the HAMP domain to the conserved linker region connecting the last α -helix of the HAMP (stalk helix) to the GGDEF domain. This in turn unlocks the C-terminal domains to form a catalytically active dimer. At that moment, c-di-GMP is formed and the increase in c-di-GMP level will trigger increased biofilm formation and reduced motility (Giardina *et al.*, 2013).

The data obtained here provides evidence that YIP interacts with the TM helices of the *P. aeruginosa* YfiN to exert its biological effect. This interaction could induce a conformational change that triggers a similar torsion of the HAMP domain to unlock the C-terminal catalytic domains, this hypothesis is depicted in the left panel of Fig. 5. As stated in literature for (over)activation of YfiN, the swarming capacity of *P. aeruginosa* was observed to suffer the most severe reduction (Malone *et al.*, 2010).

Consequences of c-di-GMP interference for phage infection

Within the context of phage biology, the role of these small peptides within their biological context is likely to be complex. Based on the initial screening approach, we used a highly reductionist approach (selection of individual phage ORFs showing a phenotypic effect) to

elucidate the role of their individual corresponding proteins. From this perspective, we provided, to our knowledge, the first example of a phage protein interfering with the c-di-GMP signalling pathway. This peptide could serve as a basis to better understand the YfiN model from a structural perspective and has potential applications towards biotechnology and antibacterial design strategies. Indeed, targeting c-di-GMP signalling has been proposed as a promising novel antibacterial strategy (reviewed by Valentini and Filloux (2019)). Yet, these c-di-GMP researches focus on decreasing intracellular c-di-GMP levels, via directly binding and sequestering c-di-GMP (Hee *et al.*, 2020) or indirectly via inhibiting DGCs or activating PDEs (reviewed by Opoku-Temeng *et al.* (2016) and Valentini and Filloux (2019)). Future work will aim at investigating the biotechnological potential of the YIP proteins. In addition, the induced production of c-di-GMP by YIP may be relevant for phage therapy applications, in which *Pbunavirus* phages are often used (Merabishvili *et al.*, 2009; Rose *et al.*, 2014).

The increase of c-di-GMP in *P. aeruginosa* upon phage 14-1 infection was indirectly observed by the significant upregulation of the genes encoding for c-di-GMP regulated proteins CdrA and CdrB, which promotes biofilm formation (Blasdel *et al.*, 2018; Borlee *et al.*, 2010). Several hypotheses can be put forward towards the biological function of YIP during phage infection. Since the infection of phage 14-1 is completed in less than 15 min in optimal conditions, it is unlikely that the expression of YIP has a direct impact on the biofilm formation capacity

of the infected cells. However, reports indicating that host populations can respond to phage infection by increasing biofilm formation have been described (Hosseinioust *et al.*, 2013; Tan *et al.*, 2015). The impact on motility can be more direct, possibly preventing bacterial swarming towards environments with a lower bacterial density or providing superinfection exclusion properties (preventing expression of virulence genes which can act as receptors for some phage) (De Smet *et al.*, 2017). Also, the complex intracellular role of c-di-GMP should be considered, as c-di-GMP is seen to affect almost every process in a bacterial cell, through transcriptional, post-transcriptional and post-translational regulation (Hengge, 2016; Valentini and Filloux, 2019). For example, c-di-GMP impacts cell cycle progression by proteolysis of a replication inhibitor (Duerig *et al.*, 2009) or switching a cell cycle kinase to phosphatase mode (Lori *et al.*, 2015), which for these phages may be of importance for a successful lytic infection cycle. Moreover, *E. coli* YfiN can block cell division by relocating and interacting with early division proteins (Kim and Harshey, 2016). This second role for YfiN may implicate that upon stimulation by YIP less energy will be put into cell growth, which for these phages might be necessary to support phage progeny production.

The importance of cell signalling in the phage infection process has only recently gained attention. Phage-mediated quorum sensing interference has been shown to regulate phage infection, providing bacterial cells resistance against upcoming phage infections and controlling the lytic-lysogenic switch in response to environmental and cell physiological changes (Erez *et al.*, 2017; Silpe and Bassler, 2019; Chung *et al.*, 2014). Moreover, the cyclic dinucleotide cGAMP in *Vibrio cholerae* is shown to induce a cellular suicide programme upon phage infection to protect the bacterial community from a viral epidemic (a mechanism known as abortive infection) (Cohen *et al.*, 2019). Furthermore, high levels of c-di-GMP are shown to be required for *E. coli* phage N4 infection, as overexpression of PDEs confer phage resistance (Mutalik *et al.*, 2020). Therefore, the discovery of our phage-encoded c-di-GMP interfering peptides YIPs expands the knowledge on the multilevel role of cell signalling in phage infection and emphasizes the importance of this still underestimated mechanism in host take-over.

Experimental procedures

Expression in P. aeruginosa and bacterial growth experiments

The phage genes were cloned using the Gateway system, as described previously (Hendrix *et al.*, 2019). Finally, the genes were cloned in the *E. coli* – *P. aeruginosa* shuttle

expression vector pUC18-mini-Tn7T-Lac-GW, which was inserted in the bacterial genome allowing single gene copy expression of the phage protein. Alternatively, the phage genes were cloned in the pME6032 expression vector to allow high-copy expression in *P. aeruginosa* PAO1 and PA14 (Heeb *et al.*, 2002). For the initial toxicity screen of the early phage genes, *P. aeruginosa* cells were grown, as previously described (Wagemans *et al.*, 2014), at 37°C in Lysogeny Broth (LB), supplemented with 0.1 mg ml⁻¹ ampicillin, 0.03 mg ml⁻¹ gentamicin and/or 1 mM IPTG, if required. The transposon mutant of *yfiN* in PAO1 (strain PW3024, genotype PA1120-C01::ISphoA/hah) was obtained from the University of Washington library (Held *et al.*, 2012). The transposon mutants of *yfiN* and *fimV* in PA14 were from the PA14NR Set (Liberati *et al.*, 2006).

Yeast two-hybrid analysis

Yeast two-hybrid analysis in *Saccharomyces cerevisiae* AH109 was performed using a random genomic fragment *P. aeruginosa* PAO1 prey library (Roucourt *et al.*, 2009), as previously described by our group (Wagemans *et al.*, 2014). Bait proteins were tested for self-activation of the HIS3, ADE2 and MEL1 reporter constructs by transformation (Gietz and Woods, 2002) of the pGBT9 phage gene bait constructs together with an empty pGAD424 prey vector or the unrelated prey Gpa1p (the α -subunit of a G protein involved in pheromone signalling in yeast). Subsequently, the bait-containing AH109 cells were transformed with the prey library following the Gietz protocol (Gietz and Schiestl, 2007). Selection of positive colonies was done using synthetic defined minimal medium as described previously (Wagemans *et al.*, 2014).

Quantification of c-di-GMP levels

The expression constructs pME6032_empty and pME6032_14-1 YIP were transformed into the c-di-GMP-responsive reporter strain of *P. aeruginosa* PAO1 (Rybtke *et al.*, 2012). The resulting strains were grown overnight in VBMM minimal medium (3 g l⁻¹ trisodium citrate, 2 g l⁻¹ citric acid, 10 g l⁻¹ K₂HPO₄, 3.5 g l⁻¹ NaNH₄PO₄·4H₂O, pH 7) supplemented with 0.1 mM CaCl₂ and 1 mM MgSO₄. Then, an aliquot of this overnight culture was re-inoculated in 3 ml fresh VBMM minimal medium and grown until an OD₆₀₀ = 0.1. At this moment, IPTG was added to half of the samples to induce expression, in total three replicas per condition were analysed. After 1.5 h of induction, 2 μ l of the culture was spotted on a VBMM agar pad and visualized with a temperature controlled (Okolab Ottaviano, Pozzuoli, NA, Italy) Ti-Eclipse inverted microscope (Nikon) equipped with a TI-CT-E motorized condenser and a

CoolSnap HQ2 FireWire CCD-camera. Images were acquired using the NIS-Elements AR 3.2 software (Nikon) as described previously (Cenens *et al.*, 2013). The average cellular fluorescence was determined using MicrobeTracker (Sliusarenko, 2012) to analyse the data.

Biofilm formation assay

Biofilm formation was assessed using the Calgary bio-film device (Ceri *et al.*, 1999). Overnight cultures were diluted 200-fold in LB medium \pm 1 mM IPTG in the 96 wells of a microtiter plate. Each plate contained four replicas per construct, arranged in a way to minimize spatial influence on biofilm formation, and three biological replicates were analysed. Once the pegs were placed in the wells, and the plate was sealed to reduce evaporation. Biofilms were then grown for 24 h at 37°C without shaking. The quantitative analysis of the biofilm formation and planktonic survival was performed as described previously (Cornelissen *et al.*, 2011). Briefly, the pegs were washed in LB, stained for 30 min with crystal violet (0.1 % crystal violet (Merck, Kenilworth, NJ, USA) in a 1:1:18 (v/v) isopropanol-methanol-PBS (phosphate-buffered saline) solution and excess crystal violet was washed from the pegs. After a 30 min fixation step, crystal violet staining is removed from the pegs using a 30% cold acetic acid solution and quantified with the Multiskan RC.

Motility assay

To assess swimming and swarming motility, bacteria were spotted and incubated for 48 h at 37°C on: swim medium (1 % (w/v) Bacto tryptone, 0.25 % (w/v) NaCl, 0.3 % (w/v) agar) and swarm medium (LB medium with 0.5 % (w/v) agar). To assess the twitching motility, the cells were stab inoculated in the middle of a plate containing LB medium with 1 % (w/v) agar and incubated for 48 h at 37°C. Then, the agar was removed, the bottom of the plate was stained with 0.01% crystal violet in a 18:1:1 solution of PBS, methanol and isopropanol for 30 min and dried by contact with air. The longest and shortest diameter of the formed halo indicative of the twitching motility activity was finally measured and the average of these values was taken. The assays were done in triplicate (swimming) and quintuplet (swarming and twitching).

Flow chamber experiment for assessing impact on biofilm 3D structure. The flow chamber system setup (DTU Health Tech, Lyngby-Taarbaek, Denmark) was used to grow biofilms as described by Weiss Nielsen *et al.* (2011). The flow chambers had a rectangular shape with a length of 40 mm, a width of 4 mm and a

height of 1 mm and encompassed a total volume of 160 μ l. The chambers contained a microscope cover glass (Menzel-Gläser, Braunschweig, Germany) as substratum for biofilm formation. The flow chambers were turned upside down and were inoculated by injecting 350 μ l of a suspension containing an equal number of *P. aeruginosa* cells with or without the pUC18-mini-TN7T-LAC YIP expression construct (at 2.5×10^8 cells ml^{-1} each) dissolved in 10 mM MgSO_4 through the connected tubing into the flow chamber using a syringe (Myjector U⁻¹00 insulin needle; Terumo, Leuven, Belgium). Bacterial cells were allowed to attach to the glass substratum for 1 h, after which the flow chambers were turned again. Three flow chambers per strain, respectively, *P. aeruginosa* with an empty expression construct and one with 14-1 YIP inserted, were then continuously irrigated at 3.5 ml h^{-1} with minimal medium for *Pseudomonas* (30 mM Na_2HPO_4 , 14 mM KH_2PO_4 , 20 mM $(\text{NH}_4)_2\text{SO}_4$, 20 mM glucose, 1 mM MgSO_4 , 4 μM FeSO_4), while three other channels per strain were irrigated with the minimal medium for *Pseudomonas* supplemented with 1 mM IPTG. After four days of incubation at 25°C, the flow chambers were disconnected at the end of the experiment for CLSM analysis of the developed biofilms.

CLSM and image analysis. Biofilms were visualized with an IX81 inverted microscope (Olympus, Tokyo, Japan) equipped with a Fluoview FV1000 confocal scanning unit (Olympus). Prior to CLSM analysis, cells in the flow chamber were stained with SYBR Green II nucleic acid gel stain (Invitrogen, Belgium) by injection of the DNA stain through the tubing in the flow chamber and subsequently incubated for 30 min. Then, three distinct CLSM images of each of the biofilms were taken at three different positions in the chambers, e.g., front, middle and back section of the chambers. Images (512 \times 512 pixel frame; 0.414 μm pixel size) were captured at 1 μm increments with a UPL SAPO \times 60/1.35 objective (Olympus). Imaris 7.2 software (Bitplane, Concord, MA, USA) was used for visualization of the biofilms.

Acknowledgements

We would like to thank prof. Tim Tolker-Nielsen (University of Copenhagen) for providing the Copenhagen c-di-GMP reporter *P. aeruginosa* strains. This work was in part supported by a GOA grant 'Phage biosystems' (GOA/15/006) from KU Leuven. J.D.S. holds a postdoctoral fellowship grant (grant number: 12V5219N) of the Research Foundation – Flanders. I.S. and A.V. hold a 'strategic basic research' PhD fellowship (grant numbers: 1S56416N and 1S44616N, respectively) of the Research Foundation – Flanders.

Conflict of Interests

The authors state that there are no competing interests to be reported.

Author contributions

J.W. carried out initial toxicity screen and Y2H. H.H. performed the cloning and testing of toxicity in transposon mutants. I.S. and J.D.S. performed (time-lapse) microscopy. J.D.S., A.V. and H.H. carried out motility and stationary biofilm formation assays. B.H. and J.D.S. carried out flow cell experiments and confocal laser scanning microscopy. J.D.S. and R.L. designed experiments. J.D.S. and H.H. wrote the manuscript, and all authors commented on the manuscript.

References

- Baraquet, C., and Harwood, C.S. (2013) Cyclic diguanosine monophosphate represses bacterial flagella synthesis by interacting with the Walker A motif of the enhancer-binding protein FleQ. *Proc Natl Acad Sci USA* **110**: 18478–18483.
- Basu, R.A., and Sauer, K. (2014) Diguanylate cyclase NicD-based signalling mechanism of nutrient-induced dispersion by *Pseudomonas aeruginosa*. *Mol Microbiol* **94**: 771–793.
- Blasdel, B.G., Ceyssens, P.-J., Chevallereau, A., Debarbieux, L., and Lavigne, R. (2018) Comparative transcriptomics reveals a conserved Bacterial Adaptive Phage Response (BAPR) to viral predation. *bioRxiv*, 248849.
- Borlee, B.R., Golman, A.D., Murakami, K., Samudrala, R., Wozniak, D.J., and Parsek, M.R. (2010) *Pseudomonas aeruginosa* uses a cyclic-di-GMP-regulated adhesion to reinforce the biofilm extracellular matrix. *Mol Microbiol* **75**: 827–842.
- Buensuceso, R.N.C., Nguyen, Y., Zhang, K., Daniel-Ivad, M., Sugiman-Marangos, S.N., Fleetwood, A. D., et al. (2016) The conserved tetratricopeptide repeat-containing C-terminal domain of *Pseudomonas aeruginosa* FimV is required for its cyclic AMP-dependent and -independent functions. *J Bacteriol* **198**: 2263–2274.
- Caly, D.L., Bellini, D., Walsh, M.A., Dow, J.M., and Ryan, R.P. (2015) Targeting cyclic di-GMP signalling: a strategy to control biofilm formation? *Curr Pharm Des* **21**: 12–24.
- Cenens, W., Mebrhatu, M.T., Makumi, A., Ceyssens, P.J., Lavigne, R., Van Houdt, R., et al. (2013) Expression of a novel P22 ORFan gene reveals the phage carrier state in *Salmonella typhimurium*. *PLoS Genet* **9**: e1003269.
- Ceri, H., Olson, M.E., Stremick, C., Read, R.R., Morck, D., and Buret, A. (1999) The Calgary Biofilm Device: new technology for rapid determination of antibiotic susceptibilities of bacterial biofilms. *J Clin Microbiol* **37**: 1771–1776.
- Ceyssens, P.-J., Miroshnikov, K., Mattheus, W., Krylov, V., Robben, J., Noben, J.-P., et al. (2009) Comparative analysis of the widespread and conserved PB1-like viruses infecting *Pseudomonas aeruginosa*. *Environ Microbiol* **11**: 2874–2883.
- Christen, M., Kulasekara, H.D., Christen, B., Kulasekara, B.R., Hoffman, L.R., and Miller, S.I. (2010) Asymmetrical distribution of the second messenger c-di-GMP upon bacterial cell division. *Science* **328**: 1295–1297.
- Chung, I.Y., Jang, H.J., Bae, H.W., and Cho, Y.H. (2014) A phage protein that inhibits the bacterial ATPase required for type IV pilus assembly. *Proc Natl Acad Sci USA* **111**: 11503–11508.
- Cohen, D., Melamed, S., Millman, A., Shulman, G., Oppenheimer-Shaanan, Y., Kacen, A., et al. (2019) Cyclic GMP-AMP signaling protects bacteria against viral infection. *Nature* **574**: 691–695.
- Cornelissen, A., Ceyssens, P.J., T'Syen, J., Van Praet, H., Noben, J.P., Shaburova, O.V., et al. (2011) The T7-related *Pseudomonas putida* phage ϕ 15 displays virion-associated biofilm degradation properties. *PLoS One* **6**: e18597.
- Duerig, A., Abel, S., Folcher, M., Nicollier, M., Schwede, T., Amiot, N., Giese, B. & Jenal, U. (2009) Second messenger-mediated spatiotemporal control of protein degradation regulates bacterial cell cycle progression. *Genes Dev.* **2393–104**.
- Erez, Z., Steinberger-Levy, I., Shamir, M., Doron, S., Stokar-Avihail, A., Peleg, Y., et al. (2017) Communication between viruses guides lysis-lysogeny decisions. *Nature* **541**: 488–493.
- Garbe, J., Wesche, A., Bunk, B., Kzamiereczak, M., Selezska, K., Rohde, C., et al. (2010) Characterization of JG024, a *Pseudomonas aeruginosa* PB1-like broad host range phage under simulated infection conditions. *BMC Microbiol* **10**: 301.
- Giardina, G., Paiardini, A., Fericola, S., Franceschini, S., Rinaldo, S., Stelitano, V., and Cutruzzola, F. (2013) Investigating the allosteric regulation of YfiN from *Pseudomonas aeruginosa*: clues from the structure of the catalytic domain. *PLoS One* **8**: e81324.
- Gietz, R.D., and Schiestl, R.H. (2007) Large-scale high-efficiency yeast transformation using the LiAc/SS carrier DNA/PEG method. *Nat Protoc* **2**: 38–41.
- Gietz, R.D., and Woods, R.A. (2002) Screening for protein-protein interactions in the yeast two-hybrid system. *Methods Mol Biol* **185**: 471–486.
- Hee, C.-S., Habazettl, J., Schumutz, C., Schirmer, T., Jenal, U., and Grzesiek, S. (2020) Intercepting second-messenger signaling by rationally designed peptides sequestering c-di-GMP. *Proc Natl Acad Sci USA* **117**: 17211–17220.
- Heeb, S., Blumer, C., and Haas, D. (2002) Regulatory RNA as mediator in GacA / RsmA-dependent global control of exoproduct formation in *Pseudomonas fluorescens* CHA0. *J Bacteriol* **184**: 1046–1056.
- Held, K., Ramage, E., Jacobs, M., Gallagher, L., and Manoil, C. (2012) Sequence-verified two-allele transposon mutant library for *Pseudomonas aeruginosa* PAO1. *J Bacteriol* **194**: 6387–6389.
- Hendrix, H., Staes, I., Aertsen, A., and Wagemans, J. (2019) Screening for growth-inhibitory ORFans in *Pseudomonas aeruginosa*-infecting bacteriophages. *Methods Mol Biol* **1898**: 147–162.

- Hengge, R. (2009) Principles of c-di-GMP signalling in bacteria. *Nat Rev Microbiol* **7**: 263–273.
- Hengge, R. (2016) Trigger phosphodiesterases as a novel class of c-di-GMP effector proteins. *Philos Trans R Soc Lond B Biol Sci* **371**: pii: 20150498.
- Hengge, R., Galperin, M.Y., Ghigo, J.-M., Gomelsky, M., Green, J., Hughes, K.T., *et al.* (2016) Systematic nomenclature for GGDEF and EAL domain-containing cyclic di-GMP turnover proteins of *Escherichia coli*. *J Bacteriol* **198**: 7–11.
- Hosseinidoust, Z., Tufenkji, N., and van den Ven, T.G.M. (2013) Formation of biofilms under phage predation: considerations concerning a biofilm increase. *Biofueling* **29**: 457–468.
- Jimenez, P.N., Koch, G., Thompson, J.A., Xavier, K.B., Cool, R.H., and Quax, W.J. (2012) The multiple signaling systems regulating virulence in *Pseudomonas aeruginosa*. *Microbiol Mol Biol Rev* **76**: 46–65.
- Kim, H.K., and Harshey, R.M. (2016) A diguanylate cyclase acts as a cell division inhibitor in a two-step response to reductive and envelope stresses. *mBio* **7**: e00822–16.
- Klausen, M., Heydorn, A., Ragas, P., Lambertsen, L., Aaes-Jørgensen, A., Molin, S., and Tolker-Nielsen, T. (2003) Biofilm formation by *Pseudomonas aeruginosa* wild type, flagella and type IV pili mutants. *Mol Microbiol* **48**: 1511–1524.
- Krogh, A., Larsson, B., von Heijne, G., and Sonnhammer, E.L. (2001) Predicting transmembrane protein topology with a hidden Markov model: application to complete genomes. *J Mol Biol* **305**: 567–580.
- Kulasakara, H., Lee, V., Brencic, A., Liberati, N., Urbach, J., Miyata, S., *et al.* (2006) Analysis of *Pseudomonas aeruginosa* diguanylate cyclases and phosphodiesterases reveals a role for bis-(3'-5')-cyclic-GMP in virulence. *Proc Natl Acad Sci USA* **103**: 2839–2844.
- Liberati, N.T., Urbach, J.M., Miyata, S., Lee, D.G., Drenkard, E., Wu, G., *et al.* (2006) An ordered, nonredundant library of *Pseudomonas aeruginosa* strain PA14 transposon insertion mutants. *Proc Natl Acad Sci USA* **103**: 2833–2838.
- Lori, C., Ozaki, S., Steiner, S., Böhm, R., Abel, S., Dubey, B. N., *et al.* (2015) Cyclic di-GMP acts as a cell cycle oscillator to drive chromosome replication. *Nature* **523**: 236–239.
- Madeira, F., Park, Y.M., Lee, J., Buso, N., Gur, T., Madhusoodanan, N., *et al.* (2019) The EMBL-EBI search and sequence analysis tools APIs in 2019. *Nucleic Acids Res* **47**: 636–641.
- Malone, J.G., Jaeger, T., Spangler, C., Ritz, D., Spang, A., Arrieumerlou, C., *et al.* (2010) YfiBNR mediates cyclic di-GMP dependent small colony variant formation and persistence in *Pseudomonas aeruginosa*. *PLoS Pathog* **6**: e1000804.
- Martinez-Granero, F., Navazo, A., Barahona, E., Redondo-Nieto, M., Gonzalez de Heredia, E., Baena, I., *et al.* (2014) Identification of flgZ as a flagellar gene encoding a PilZ domain protein that regulates swimming motility and biofilm formation in *Pseudomonas*. *PLoS One* **9**: e87608.
- Massie, J.P., Reynolds, E.L., Koestler, B.J., Cong, J.P., Agostoni, M., and Waters, C.M. (2012) Quantification of high-specificity cyclic diguanylate signaling. *Proc Natl Acad Sci USA* **109**: 12746–12751.
- Merabishvili, M., Pirnay, J.-P., Verbeken, G., Chanishvili, N., Tediashvili, M., Lashkhi, N., *et al.* (2009) Quality-controlled small-scale production of a well-defined bacteriophage cocktail for use in human clinical trials. *PLoS One* **4**: e4944.
- Merritt, J.H., Brothers, K.M., Kuchma, S.L., and O'Toole, G.A. (2007) SadC reciprocally influences biofilm formation and swarming motility via modulation of exopolysaccharide production and flagellar function. *J Bacteriol* **189**: 8154–8164.
- Merritt, J.H., Ha, D.G., Cowles, K.N., Lu, W., Morales, D.K., Rabinowitz, J., *et al.* (2010) Specific control of *Pseudomonas aeruginosa* surface-associated behaviors by two c-di-GMP diguanylate cyclases. *mBio* **1**: e00183–10.
- Mutalik, V.K., Adler, B.A., Rishi, H.S., Piya, D., Zhong, C., Koskella, B., *et al.* (2020) High-throughput mapping of the phage resistance landscape in *E. coli*. *Plos Biol* **18**: e3000877.
- Opoku-Temeng, C., Zhou, J., Zheng, Y., Su, J., and Sintim, H.O. (2016) Cyclic dinucleotide (c-di-GMP, c-di-AMP, and cGAMP) signaling have come of age to be inhibited by small molecules. *Chem Commun* **52**: 9327–9342.
- Pesavento, C., and Hengge, R. (2009) Bacterial nucleotide-based second messengers. *Curr Opin Microbiol* **12**: 170–176.
- Petrova, O.E., Cherny, K.E., and Sauer, K. (2015) The diguanylate cyclase GcbA facilitates *Pseudomonas aeruginosa* biofilm dispersion by activating BdlA. *J Bacteriol* **197**: 174–187.
- Petrova, O.E., and Sauer, K. (2012) Dispersion by *Pseudomonas aeruginosa* requires an unusual posttranslational modification of BdlA. *Proc Natl Acad Sci USA* **109**: 16690–16695.
- Römling, U., Galperin, M.Y., and Gomelsky, M. (2013) Cyclic di-GMP: the first 25 years of a universal bacterial second messenger. *Microbiol Mol Biol Rev* **77**: 1–52.
- Rose, T., Verbeken, G., De Vos, D., Merabishvili, M., Vaneechoutte, M., Lavigne, R., *et al.* (2014) Experimental phage therapy of burn wound infection: difficult first steps. *Int J Burns Trauma* **4**: 66–73.
- Ross, P., Weinhouse, H., Aloni, Y., Michaeli, D., Weinberger-Ohana, P., Mayer, R., *et al.* (1987) Regulation of cellulose synthesis in *Acetobacter xylinum* by cyclic diguanylic acid. *Nature* **325**: 279–281.
- Roucort, B., Lecoutere, E., Chibeu, A., Hertveldt, K., Volckaert, G., and Lavigne, R. (2009) A procedure for systematic identification of bacteriophage-host interactions of *P. aeruginosa* phages. *Virology* **387**: 50–58.
- Ryan, R.P. (2013) Cyclic di-GMP signalling and the regulation of bacterial virulence. *Microbiology* **159**: 1286–1297.
- Rybtke, M.T., Borlee, B.R., Murakami, K., Irie, Y., Hentzer, M., Nielsen, T.E., *et al.* (2012) Fluorescence-based reporter for gauging cyclic di-GMP levels in *Pseudomonas aeruginosa*. *Appl Environ Microbiol* **78**: 5060–5069.
- Seshasayee, A.S., Fraser, G.M., and Luscombe, N.M. (2010) Comparative genomics of cyclic-di-GMP signaling in bacteria: post-translational regulation and catalytic activity. *Nucleic Acids Res* **38**: 5970–5981.
- Silpe, J.E., and Bassler, B.L. (2019) A host-produced quorum-sensing autoinducer controls a phage lysis-lysogeny decision. *Cell* **176**: 268–280.e13.

- Simm, R., Morr, M., Kader, A., Nimtz, M., and Römling, U. (2004) GGDEF and EAL domains inversely regulate cyclic di-GMP levels and transition from sessility to motility. *Mol Microbiol* **53**: 1123–1134.
- Sliusarenko, O. (2012) Microbetracker software. *Mol. Microbiol.* **80**: 612–627.
- De Smet, J., Hendrix, H., Blasdel, B.G., Danis-Wlodarczyk, K., and Lavigne, R. (2017) *Pseudomonas predators*: understanding and exploiting phage-host interactions. *Nat Rev Microbiology* **15**: 517–530.
- Tan, D., Dahl, A., and Middelboe, M. (2015) Vibriophages differentially influence biofilm formations by *Vibrio anguillarum* strains. *Appl Environ Microbiol* **81**: 4489–4497.
- Ueda, A., and Wood, T.K. (2009) Connecting quorum sensing, c-di-GMP, pel polysaccharide, and biofilm formation in *Pseudomonas aeruginosa* through tyrosine phosphatase TpbA (PA3885). *PLoS Pathog* **5**: e1000483.
- Valentini, M., and Filloux, A. (2016) Biofilms and cyclic di-GMP (c-di-GMP) signaling: lessons from *Pseudomonas aeruginosa* and other bacteria. *J Biol Chem* **291**: 12547–12555.
- Valentini, M., and Filloux, A. (2019) Multiple roles of c-di-GMP signaling in bacterial pathogenesis. *Annu Rev Microbiol* **73**: 387–406.
- Van den Bossche, A., Ceysens, P.J., De Smet, J., Hendrix, H., Bellon, H., Leimer, N., et al. (2014) Systematic identification of hypothetical bacteriophage proteins targeting key protein complexes of *Pseudomonas aeruginosa*. *J Proteome Res* **13**: 4446–4456.
- van Schaik, E.J., Giltner, C.L., Audette, G.F., Keizer, D.W., Bautista, D.L., Slupsky, C.M., et al. (2005) DNA binding: a novel function of *Pseudomonas aeruginosa* type IV pili. *J Bacteriol* **187**: 1455–1464.
- Wagemans, J., Blasdel, B.G., Van den Bossche, A., Uytterhoeven, B., De Smet, J., Paeshuyse, J., et al. (2014) Functional elucidation of antibacterial phage ORFans targeting *Pseudomonas aeruginosa*. *Cell Microbiol* **16**: 1822–1835.
- Wagemans, J., Delattre, A.S., Uytterhoeven, B., De Smet, J., Cenens, W., Aertsen, A., et al. (2015) Antibacterial phage ORFans of *Pseudomonas aeruginosa* phage LUZ24 reveal a novel MvaT inhibiting protein. *Front Microbiol* **6**: 1242.
- Wan, X., Hendrix, H., Skurnik, M., and Lavigne, R. (2020) Phage-based target discovery and its exploitation towards novel antibacterial molecules. *Curr Opin Biotechnol* **68**: 1–7.
- Wehbi, H., Portillo, E., Harvey, H., Shimkoff, A.E., Scheurwater, E.M., Howell, P.L., and Burrows, L.L. (2011) The peptidoglycan-binding protein FimV promotes assembly of the *Pseudomonas aeruginosa* Type IV pilus secretin. *J Bacteriol* **193**: 540–550.
- Weiss Nielsen, M., Sternberg, C., Molin, S., and Regenber, B. (2011) *Pseudomonas aeruginosa* and *Saccharomyces cerevisiae* biofilm in flow cells. *J Vis Exp* **47**: 2383.
- Zhang, Z., Schwartz, S., Wagner, L., and Miller, W. (2000) A greedy algorithm for aligning DNA sequences. *J Comput Biol* **7**: 203–214.

Supporting information

Additional supporting information may be found online in the Supporting Information section at the end of the article.

Fig. S1. *In silico* transmembrane analysis of 14-1 gp11/YIP. Transmembrane helices prediction using the TMHMM webtool (Krogh et al., 2001).

Fig. S2. Confirmation test for the LBL3 YIP interactions. A. *Saccharomyces cerevisiae* AH109 cells co-expressing the indicated combinations of constructs were plated on selective SD medium lacking tryptophan and leucine (selecting for the presence of the two plasmids) (-WL), and SD medium without tryptophan, leucine, histidine and adenine but supplemented with X- α -Gal (extra selection for the activation of the *HIS3*, *ADE2* and *MEL1* reporters) (-WLHA + X- α -Gal). LBL3 YIP interacts with *Pseudomonas* proteins YfiN and FimV, as indicated by the ability to grow on selective SD-WLHA + X- α -gal medium. The cells are white to pale blue when grown on X- α -Gal supplemented medium, indicating weak interactions. B. Validation of the Y2H screen. Presence of bait and preys was verified on selective medium lacking tryptophan and leucine (SD-WL). Interactions between bait and prey were identified on selective medium without tryptophan, leucine and histidine (extra selection for the activation of the *HIS3*) (SD-WLH). The growth of fresh yeast cells expressing YIP as bait and YfiN or FimV as prey on SD-WLH medium confirms previously observed interactions. As negative controls, the YIP bait, YfiN prey and FimV prey were tested for autoactivation using Gpa1p and the empty vector as prey/bait. No growth was observed on selective SD-WLH medium. As positive control, the Mip – MvaT interaction (Wagemans et al., 2015) was added.

Fig. S3. Impact of 14-1 YIP on bacterial growth in *P. aeruginosa* PA14 wt, *yfiN::Tn* and *fimV::Tn*. Tenfold serial dilutions of *P. aeruginosa* PA14 cells containing multi-copy pME6032 plasmid with inserted YIP gene (14-1 gp11) under control of an IPTG-inducible promoter, were spotted on LB agar without (left) or with (right) 1 mM IPTG and grown for 40 h at 37°C. As negative controls, *P. aeruginosa* PA14 strains with empty pME6032 vector were used. YIP triggers a phenotypic effect of reduced spreading of the colony in both PA14 wt and the PA14 transposon mutant of *fimV* (*fimV::Tn*). The observed phenotypic effect of the YIP protein is absent in the PA14 transposon mutant of *yfiN* (*yfiN::Tn*), showing that this protein could indeed be the direct target of YIP.

Table S1. Multiple sequence alignment of homologous peptides of 14-1 gp11/YIP. The nucleotide sequence of 14-1 gp11 (NC_011703) was used as a query in tBLASTx (NCBI) to identify sequences in the Nucleotide collection database (GenBank + EMBL+DDBJ + PDB+ RefSeq sequences) that encode for similar peptides. Positive hits were aligned with Clustal Omega (Madeira et al., 2019). An asterisk indicates a position which has a conserved residue. A colon and a period indicate a conservation between a group of strongly and weakly similar amino acids, respectively. The residues marked in red are small, hydrophobic amino acids, those labelled magenta are basic amino acids, whereas the other amino acids are marked in green. The peptides studied in

this work are indicated in bold. In total, 97 homologs were identified, all belonging to *Pbunavirus* phages and containing 16 conserved residues, except for phage anti-nowhere, which misses the first three amino acids.

Table S2. Y2H library screening of LBL3 YIP against a *P. aeruginosa* PAO1 random fragment prey library. For each identified prey protein fragment, the frequency of occurrence (Freq.) in the colonies positive for all three

reporter constructs and the length (in number of amino acids) of the inserted polypeptide is listed together with the corresponding *P. aeruginosa* PAO1 protein. [§] A negative start value (between brackets) indicates part of the 5' non-coded sequence is included in the in-frame fusion construct and the corresponding prey protein, resulting in a linker between the fusion protein.